

Modelling the PHC-char separator for the PYSOLO solar integrated pyrolysis plant

Prussi M. ^{1,*}, Danesh P. ¹, Rizzo A.M. ², Lombardi J. ², Chiamomonti D. ^{1,2}

¹ DENERG (Department of ENERGY), Politecnico di Torino, C.so Duca degli Abruzzi, 10129, Turin (IT)

² Renewable Energy Consortium (RE-CORD), V.le Kennedy 182, 50038 Scarperia (IT)

*Corresponding author: matteo.prussi@polito.it

ABSTRACT: The EU supported PYSOLO project aims at investigating a pyrolysis reactor with Concentrating Solar Power (CSP) technology, to enhance biomass conversion and reduced process energy demand. As part of this project, a comprehensive numerical model has been proposed to describe the dynamics of a separator, fed by a mixture of Particles Heat Carrier (PHC) and char. This model supports the design of efficient separation systems, which will be tested under both cold and hot conditions with dedicated experimental setups. The separation concept uses fluidized bed technology in a dense zone, leveraging on the biochar and PHC particles density differences. The numerical modelling aims at defining the best operative conditions, including but not limited to gas phase velocity, char and heat carrier properties and dimensional distributions, etc.

Keywords: biochar, pyrolysis, separator, fluidized bed

1 INTRODUCTION

Biomass can result in zero or even negative-carbon fuels, today accounting for about the 10% of the world's energy demand, with a projected 28% increase in biofuel demand over the next five years [1], [2]. Pyrolysis technologies play a critical role, being able to convert low-heat-value biomass into energy-dense bio-oil and biochar [3]. The production of bio-products in fast pyrolysis, making use of auger pyrolyzers, are today a versatile and promising technology for bioenergy [4]. These reactors employing particle heat carriers (PHCs), such as sand, to facilitate uniform heating and thermal stability, thereby enabling the efficient conversion of biomass [5]. During pyrolysis process, heavier and larger carbon particles may remain within the reactor, leading to lower bio-oil yields [6]. In general, designing a proper separation method between biochar and heat carrier is key. Additionally, the effectiveness of such a device directly affects the following step of PHC recirculation into the pyrolyzer. Nonetheless, separating the heat carrier from the biochar is often problematic, and typical methods involve regeneration of the heat carrier through the combustion of the biochar [7].

However, this configuration may result in ash accumulation, which could diminish the liquid yield [8], and in general, promotes PHC ageing. Consequently, the targeted separation of biochar in pyrolysis systems could improve both the yield and quality of bio-oil while optimizing the utilization of biochar for various beneficial purposes.

Particle separation technologies, applied to fast pyrolysis, involve both mechanical and non-mechanical methods. Mechanical methods like centrifugation and vibrating screens [9]. Non-mechanical approaches primarily utilize fluidized beds [10]. Studies like those by Azimi et al. and Oshitani et al. [11], [12] explore optimizing fluidized beds through operational adjustments, yet challenges remain in achieving uniform particle distribution and managing continuous separation processes.

This study, which is part of the PYSOLO project (Fig. 1), proposes a correlative model for a char separator, aiming to facilitate a continuous, swift, and effective separation. The steady-state model investigates the impact of particle size distribution, minimum fluidization velocities, and superficial gas velocity, on enhancing the separation efficiency between heat carriers (HC) and biochar (BC), to select the most appropriate PHC for the PYSOLO project.

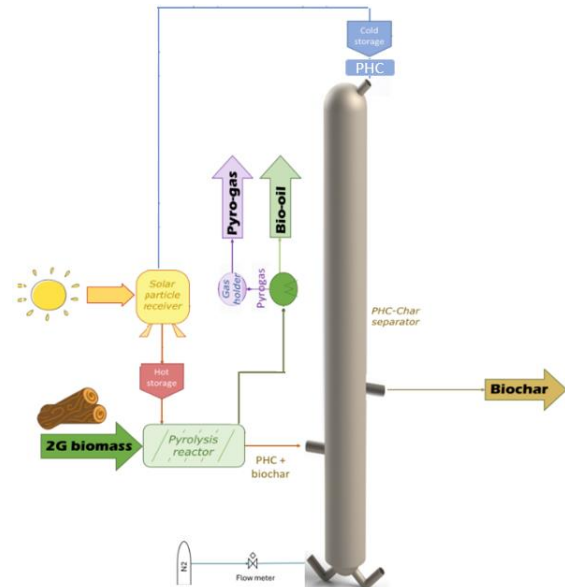


Figure 1: Conceptual configuration of biomass pyrolysis by concentrated Solar power (PYSOLO)

2 DEFINITION OF PARTICLE VERTICAL VELOCITY

2.1 Minimum fluidization velocity (U_{mf})

The Minimum fluidization velocity (U_{mf}) represents the flow velocity at which particles begin to fluidize, around the packed bed. Different correlations including experimental and theoretical are available in literature to describe the phenomenon (Table. I).

Table I: The most 8 frequent experimental and theoretical formula for minimum fluidization velocity in literature

Literature source	Experimental formula
[13]	$U_{mf} = \frac{\mu}{D_p \cdot \rho_f} \left[\sqrt{22.1^2 + 0.0354 \frac{D_p^3 \cdot \rho_f (\rho_p - \rho_f) g}{\mu^2}} - 22.1 \right]$
[14]	$U_{mf} = 1.78 \left(\frac{(1 - \epsilon) \cdot \rho_f \cdot g \cdot D_p^3 (\rho_p - \rho_f)}{\mu^2} \right)^{0.14}$
[15]	$U_{mf} = \left(\frac{\rho_p - \rho_f}{\rho_f} \right)^{0.5} \cdot \left(\frac{18\mu}{\rho_f \cdot D_p} \right)^{0.5} \cdot D_p^{1.14}$
[16]	$U_{mf} = \left[(27.32 + 0.0434 \frac{D_p^3 \cdot \rho_f \cdot (\rho_p - \rho_f) g}{\mu^2})^{0.5} \right] \frac{\mu f}{D_p \cdot \rho_f}$
[17]	$U_{mf} = \frac{D_p^2 \cdot (\rho_p - \rho_f) g}{1659 \mu f}$
Literature source	Theoretical formula
[18]	$U_{mf} = \frac{\epsilon \cdot (\rho_p - \rho_f) \cdot g \cdot D_p^2}{180 \cdot (1 - \epsilon) \cdot \mu f}$
[19]	$U_{mf} = \frac{\epsilon^3 (\rho_p - \rho_f) \cdot g \cdot D_p^2 \cdot \phi_s^2}{150 \cdot (1 - \epsilon) \cdot \mu f}$
[20]	$U_{mf} = \sqrt{\frac{\phi_s \cdot D_p \cdot (\rho_p - \rho_f) \cdot g \cdot \epsilon^3}{1.75 \cdot \rho_p}}$

Zhang et al, [20] proposed a formula, derived from Ergun equation, which resulted particularly suitable for fluidized beds of non-cohesive particles (typically where particle-particle interactions are negligible compared to particle-fluid interactions). Minimum fluidization velocity is described as formula 1:

$$U_{mf} = \sqrt{\frac{\phi_s \cdot D_p \cdot (\rho_p - \rho_f) \cdot g \cdot \epsilon^3}{1.75 \cdot \rho_p}} \quad (1)$$

The term ϕ_s represents the Sphericity of the particles, D_p is Diameter of the particles, ρ_p is Density of the particles, ρ_f is Density of the fluid, g is the gravity and ϵ is the Void fraction or porosity at minimum fluidization for high air flow.

2.2 Terminal velocity (U_t)

Terminal velocity is used to define a flow field where a particle quickly reaches a constant velocity, which is the maximum attainable under the steady-state equilibrium. The calculation of the terminal velocity considering the equilibrium among the drag force, buoyancy and gravity, as represented by the formula 2 which is called Archie-Kenney equation [21]:

$$U_t = \sqrt{\frac{4 \cdot g \cdot D_p \cdot (\rho_p - \rho_f)}{3 \cdot C_d \cdot \rho_f}} \quad (2)$$

where C_d is the drag coefficient.

2.3 Superficial gas velocity (U_g)

It is defined as the velocity at which a gas would move through a porous media or packed beds. It will be calculated considering different parameters of separation, to understand and predict the behaviour of the gas phase in the presence of solid phases.

2.4 Separation efficiency (Cumulative mass percentage)

The percentage of separation efficiency is defined as the

mass percentage of the target solid (i.e. biochar) which can be collected from the bottom of the vertical tube (see formula. 3), as function of the superficial gas velocity (air flow).

$$\text{Separation efficiency (\%)} = \frac{\text{Mass of biochar recovered}}{\text{Total mass of biochar}} \% \quad (3)$$

3 METHODOLOGICAL APPROACHES

3.1 Materials

In the framework of the PYSOLO project, the RE-CORD consortium team experimentally identified four materials potentially suitable as particle heat carriers (PHCs) (Table. II), with the relative characteristics. Biomass feed rate (fixed): 1.5 kg/h and PHC to biomass volume ratio within 0.75-1.5. The primary objective of this research is to enhance the efficiency of production yield by effectively separating PHCs from biochar in fast pyrolysis.

Table II: Physical characteristics of biochar and particle heat carriers

Material	Diameter (mm)	Particle Density (kg/m ³)	Thermal Conductivity (W/m·K)
Sand	0.1-0.4	~2000	1.14
Sintered Bauxite	0.1-0.7	~3500	2
Steel spheres	1-50	~8000	16
CaO	0.1-1	~1600	0.7
Biochar	0.1-50	400	0.2-0.3

3.2 Proposed methodological approach

This study proposes a theoretical assessment for a novel separation method, based on a fluidized bed where different gas velocities may be used to exploit the density differences between biochar and PHC particles. The method involves several key steps: evaluating the fluidization characteristics within the separator, and adjusting operational parameters (minimum fluidization, terminal, and superficial gas velocity).

Numerical modeling is used to understand the airflow dynamics over binary particles. Comparative analysis for different heat carriers' separation efficiencies will also be conducted. The key parameters considered include particle density, size, terminal velocity, particle Reynolds number, minimum fluidization velocity.

The goal is to find the optimal superficial gas velocity (U_g) for achieving a high separation rate. This optimal gas velocity will be between the terminal velocities of the heat carrier (U_{tc}) and biochar (U_{tb}): $U_{tc} < U_g < U_{tb}$.

In this study, biochar along with one of the heat carriers as binary particles, enters the separator after the pyrolysis process. Biochar-sand, biochar-bauxite, biochar-steel and biochar-calcium oxide will be modeled based on their physical characteristics.

The expected particle size distribution (PSD) of each materials is presented in Fig. 2, which providing a detailed representation of the percentage distribution of particle diameters. This figure is essential for understanding the granularity and size variability of the particles involved in the study, detailing the complexity of realising an

effective separation.

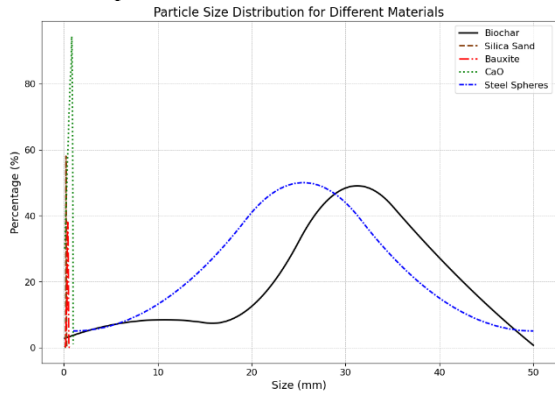


Figure 2: Particle size distribution of materials

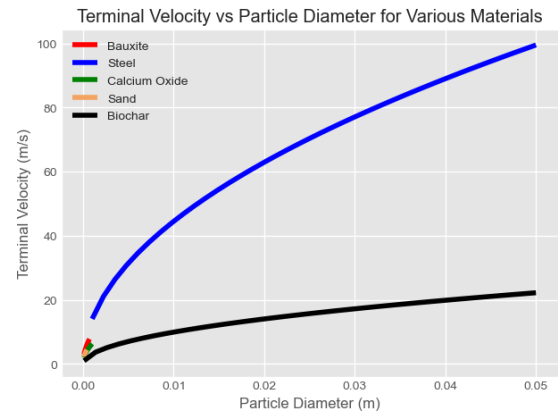


Figure 4: Terminal velocity of different particles

4 RESULT AND DISCUSSION

4.1 Minimum fluidization velocity

The calculation for the minimum fluidization velocity (U_{mf}) is presented in Fig. 3 using established parameters and assumptions commonly used for fluidized bed systems (i.e. air density is fixed at 1.2 kg/m^3 , etc.). A void fraction of 0.5 is used, representing an average for loosely packed particle beds. Additionally, particles are assumed to be perfectly spherical ($\phi_s = 1$) simplifying the calculations by eliminating the need for complex shape-related adjustments.

These parameters form the basis for theoretical calculations essential for designing and optimizing fluidized bed reactors, with predictions of fluidization dynamics crucial for enhancing process efficiency.

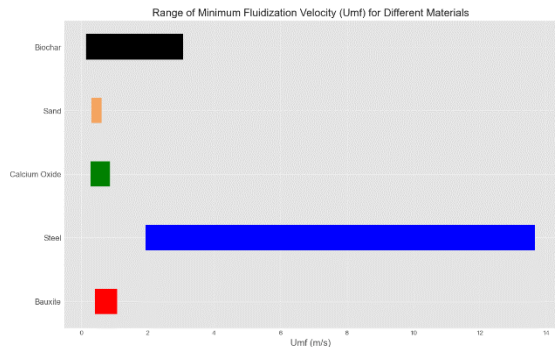


Figure 3: Minimum fluidization velocity of particles

The plot shows that sand has the lowest minimum fluidization velocity (U_{mf}) at maximum 0.61 m/s , while steel has the highest U_{mf} at 13.66 m/s due to its higher density (8000 kg/m^3). This illustrates that denser materials require higher fluid velocities to achieve fluidization state.

4.2 Terminal velocity

As shown in Fig. 4, the biochar particles require an airflow higher than 20 m/s to reach the top of the tube. Conversely, all the sand particles need an airflow of more than 4.45 m/s to be at the top. These differences are primarily due to the range of densities and sizes of the particles, which affect their drag force and terminal velocity.

5 CONCLUSIONS

Given all the defined parameters, the separation efficiency is reported in Figure 5. This plot illustrates the mass percentage of biochar with different cumulative mass distributions as a binary particle mixture in a vertical tube.

Using Calcium oxide (CaO), Bauxite, and sand as heat carriers, the separation efficiencies for biochar were tested at different superficial gas velocities.

The results showed:

- 90% efficiency for biochar from CaO at 6.29 m/s
- 87.5% efficiency for biochar from Bauxite at 7.78 m/s
- 95% efficiency for biochar from sand at 4.45 m/s

The separation efficiencies were calculated: denser materials, such as steel spheres, used as PHC, remains at the bottom and the biochar separation efficiency reached 100% at the top.

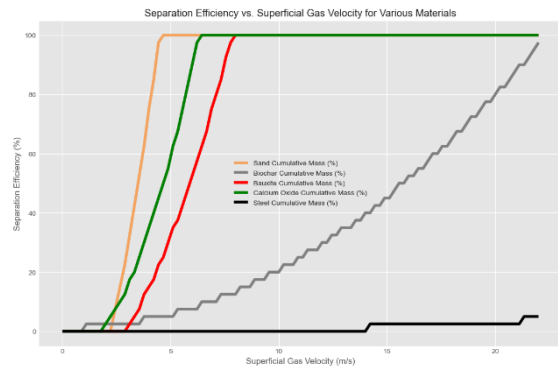


Figure 5: Separation efficiency of different particles

The theoretical terminal velocity was validated against the literature, achieving an R^2 value of 0.89 (Fig. 6).

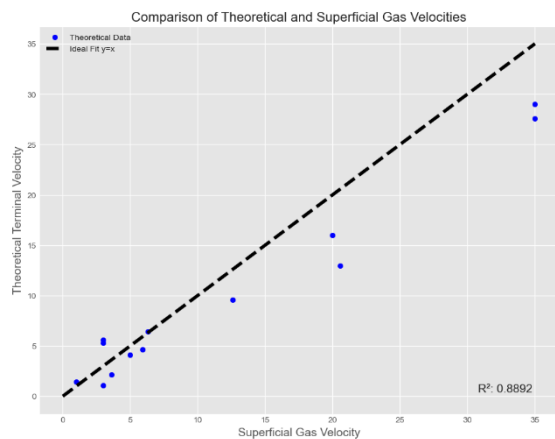


Figure 6: Validation of calculated terminal velocity

6 REFERENCES

- [1] “bp Statistical Review of World Energy 2022 (71st Edition) - BIEE.” Accessed: May 14, 2024. [Online]. Available: <https://www.biee.org/bp-statistical-review-of-world-energy-2022-71st-edition/>
- [2] K. K. Yadav *et al.*, “Review on Evaluation of Renewable Bioenergy Potential for Sustainable Development: Bright Future in Energy Practice in India,” *ACS Sustain Chem Eng*, vol. 9, no. 48, pp. 16007–16030, Dec. 2021, doi: 10.1021/ACSSUSCHEMENG.1C03114/ASSET/IMAGES/LARGE/SC1C03114_0014.JPEG.
- [3] R. Kumar *et al.*, “Lignocellulose Biomass Pyrolysis for Bio-Oil Production: Biomass Pre-treatment Methods for Production of Drop-In Fuels,” *Biowaste and Biomass in Biofuel Applications*, pp. 123–196, Jan. 2023, doi: 10.1201/9781003265597-8.
- [4] P. Brassard, S. Godbout, and V. Raghavan, “Pyrolysis in auger reactors for biochar and bio-oil production: A review,” *Biosyst Eng*, vol. 161, pp. 80–92, Sep. 2017, doi: 10.1016/J.BIOSYSTEMSENG.2017.06.020.
- [5] J. N. Brown and R. C. Brown, “Process optimization of an auger pyrolyzer with heat carrier using response surface methodology,” *Bioresour Technol*, vol. 103, no. 1, pp. 405–414, Jan. 2012, doi: 10.1016/J.BIORTECH.2011.09.117.
- [6] W. A. Razaq, M. Golonka, M. Scholz, and A. Białowiec, “Opportunities and Challenges of High-Pressure Fast Pyrolysis of Biomass: A Review,” *Energies 2021, Vol. 14, Page 5426*, vol. 14, no. 17, p. 5426, Aug. 2021, doi: 10.3390/EN14175426.
- [7] M. Sharifzadeh *et al.*, “The multi-scale challenges of biomass fast pyrolysis and bio-oil upgrading: Review of the state of art and future research directions,” *Prog Energy Combust Sci*, vol. 71, pp. 1–80, Mar. 2019, doi: 10.1016/J.PECS.2018.10.006.
- [8] M. Raza *et al.*, “Progress of the Pyrolyzer Reactors and Advanced Technologies for Biomass Pyrolysis Processing,” *Sustainability 2021, Vol. 13, Page 11061*, vol. 13, no. 19, p. 11061, Oct. 2021, doi: 10.3390/SU131911061.
- [9] S. Scholarship@western, M. O. Adegboye, and B. Franco, “2:00 AM Continuous Segregation and Removal of Biochar from Bubbling Continuous Segregation and Removal of Biochar from Bubbling Fluidized Bed Fluidized Bed,” 2013, Accessed: May 14, 2024. [Online]. Available: <https://ir.lib.uwo.ca/etd://ir.lib.uwo.ca/etd/1826>
- [10] M. Zhou *et al.*, “Investigation of Particle Motion in a Dry Separation Fluidized Bed Using PEPT,” *Minerals 2023, Vol. 13, Page 254*, vol. 13, no. 2, p. 254, Feb. 2023, doi: 10.3390/MIN13020254.
- [11] E. Azimi, S. Karimipour, Z. Xu, J. Szymanski, and R. Gupta, “Statistical Analysis of Coal Beneficiation Performance in a Continuous Air Dense Medium Fluidized Bed Separator,” *International Journal of Coal Preparation and Utilization*, vol. 37, no. 1, pp. 12–32, Jan. 2017, doi: 10.1080/19392699.2015.1123155.
- [12] J. Oshitani, R. Sugo, Y. Mawatari, T. Tsuji, Z. Jiang, and G. V. Franks, “Dry separation of fine particulate sand mixture based on density-segregation in a vibro-fluidized bed,” *Advanced Powder Technology*, vol. 31, no. 9, pp. 4082–4088, Sep. 2020, doi: 10.1016/J.APT.2020.08.016.
- [13] Z. Zhiping, N. Yongjie, and L. Qinggang, “Effect of pressure on minimum fluidization velocity,” *Journal of Thermal Science*, vol. 16, no. 3, pp. 264–269, Aug. 2007, doi: 10.1007/S11630-007-0264-2/METRICS.
- [14] D. Kunii and O. Levenspiel, *Fluidization Engineering 2nd Edition*. 2013. Accessed: May 20, 2024. [Online]. Available: <http://www.sciencedirect.com/5070/book/9780080506647/fluidization-engineering>
- [15] “Richardson Zaki Sedimentation and Fluidisation Part I PDF | PDF | Viscosity | Drag (Physics).” Accessed: May 20, 2024. [Online]. Available: <https://www.scribd.com/document/193349320/Richardson-Zaki-Sedimentation-and-Fluidisation-Part-I-pdf>
- [16] H. Zhang, Y. Huang, X. An, A. Yu, and J. Xie, “Numerical prediction on the minimum fluidization velocity of a supercritical water fluidized bed reactor: Effect of particle size distributions,” *Powder Technol*, vol. 389, pp. 119–130, Sep. 2021, doi: 10.1016/J.POWTEC.2021.05.015.
- [17] T. R. Rao and J. V. Ram. Bheemarasetti, “Minimum fluidization velocities of mixtures of biomass and sands,” *Energy*, vol. 26, no. 6, pp. 633–644, 2001, doi: 10.1016/S0360-5442(01)00014-7.
- [18] “Particle technology learning resources - Book Download.” Accessed: May 20, 2024. [Online]. Available: https://www.particles.org.uk/particle_technology_book/index.htm
- [19] R. Timsina, R. K. Thapa, B. M. E. Moldestad, and M. S. Eikeland, “Effect of particle size on flow behavior in fluidized beds,” *International Journal of Energy Production and Management*, vol. 4, no. 4, pp. 287–297, Nov. 2019, doi: 10.2495/EQ-V4-N4-287-297.
- [20] Q. Zhang, L. Fu, G. Xu, and D. Bai, “Temperature influence on minimum fluidization velocity: Complexity, mechanism, and

- solutions,” *Particuology*, vol. 88, pp. 344–349, May 2024, doi: 10.1016/J.PARTIC.2023.10.008.
- [21] A. A. Boateng, *Rotary Kilns: Transport Phenomena and Transport Processes: Second Edition*. Elsevier Inc., 2015. doi: 10.1016/C2014-0-01966-1.